

## Carbonate ion disorder in synthetic and biogenic magnesian calcites: a Raman spectral study

WILLIAM D. BISCHOFF,<sup>1</sup> SHIV K. SHARMA AND FRED T. MACKENZIE

Department of Oceanography  
and Hawaii Institute of Geophysics  
Honolulu, Hawaii 96822

### Abstract

Raman spectra of a series of synthetic and biogenic magnesian calcites with compositions up to 25 mol% MgCO<sub>3</sub>, calcite, dolomite and magnesite were recorded. Raman bands in the spectra of synthetic magnesian calcites generally show linear changes in frequency from calcite to dolomite or magnesite, but positive and negative deviations exist for the  $\nu_3$  and translational lattice modes, respectively. A synthetic sample of 25 mol% MgCO<sub>3</sub> shows anomalously low frequency values of lattice modes. Halfwidths of the Raman bands increase smoothly with magnesium concentration in synthetic phases.

Bands in the spectra of biogenic magnesian calcites generally show an increase in frequency with increasing magnesium concentration, but the variation is not as smooth as in synthetic phases. Halfwidths of Raman bands of biogenic phases are nearly always larger than those of synthetic phases. Lattice bands of biogenic materials are commonly degraded. Many of the biogenic specimens show anomalously low frequencies of lattice modes in their Raman spectra. HCO<sub>3</sub><sup>-</sup> is present in several biogenic phases as determined by the presence of a Raman band at  $\sim 1014\text{ cm}^{-1}$ .

The increasing halfwidth of Raman bands with magnesium concentration probably results from increasing positional disorder (rotation of CO<sub>3</sub><sup>2-</sup> out of the basal plane) in both synthetic and biogenic magnesian calcites. This disorder has not heretofore been recognized in magnesian calcites. The amount of disorder is a smooth function of magnesium concentration in synthetic phases but is irregular in biogenic phases. The interpretation of positional disorder as a mechanism for the halfwidth behavior of Raman bands is also supported by the behavior of unit cell *c/a* axial ratios.

### Introduction

Magnesian calcites are an important mineral component of modern and Pleistocene carbonate sediments (Land, 1967). These phases are found principally in the skeletons of marine invertebrates and as cements (Chave, 1954a, 1954b; Bathurst, 1975). Magnesian calcites of biogenic origin have been the major materials used to interpret the thermodynamic and kinetic behavior of these phases at earth-surface temperatures and pressures (Mackenzie et al., 1983). There is little information, however, concerning the crystal chemistry of biogenic and inorganic magnesian calcites. Information concerning the microstructures and associated chemical heterogeneities of these phases is essential for interpretation of their reactivity and stability (Reeder, 1983). This knowledge is necessary if we are to understand the role of magnesian calcites in geochemical processes of diagenesis, invertebrate calcification, cement formation and dissolution, and seawater chemistry.

We are currently investigating the chemistry and mineralogy of magnesian calcites by comparison of the proper-

ties of synthetic and natural materials using a variety of analytical techniques including X-ray diffraction, atomic absorption, electron microprobe, scanning and transmission electron microscopy, and infrared and Raman spectroscopy. These investigations are necessary to characterize fully synthetic and natural phases and to form a basis for interpretation of magnesian calcite stabilities from dissolution and calorimetric measurements (Mackenzie et al., 1983).

We present here the first Raman spectra obtained for magnesian calcites and give spectra from biogenic and synthetic materials for comparison. Although Raman spectra cannot be used to assess quantitatively MgCO<sub>3</sub> concentration, they can give much information about the structural behavior of the carbonate ion. Our results suggest that the carbonate ion in synthetic and biogenic magnesian calcites is disordered.

### Band assignments

Successful assignments of first-order Raman bands to the internal vibrations of carbonate ions in rhombohedral carbonates (space group  $R\bar{3}c$ ,  $Z = 2$ ) have been accomplished by factor group analysis (Bhagavantam and Venkataray-

<sup>1</sup> Present address: Department of Geology, Wichita State University, Wichita, Kansas 67208.

udu, 1939; Krishnan, 1945; Porto et al., 1966; Rutt and Nicola, 1974; White, 1974a). Raman-active modes of vibration, symmetry assignments and frequencies of vibration for rhombohedral carbonates are illustrated in Figure 1. Second-order Raman bands, those arising from overtones and combinations of the first-order Raman bands, also occur in rhombohedral carbonates (Krishnan, 1945; Krishnamurti, 1957). One of the strongest of these occurs at  $1700\text{--}1765\text{ cm}^{-1}$  and is an overtone of the infrared-active,  $2 \times \nu_2$  ( $A_{2u}$ ) mode, as described by Krishnan (1945) and Krishnamurti (1957). It is not, however, a combination of  $A_{1g}$  and  $E_g$  as described by Rutt and Nicola (1974).

Band assignments of lattice modes are equivocal. In a spectral study of calcite and dolomite, Couture (1947) attributed the lower frequency, lower intensity band ( $155\text{--}235\text{ cm}^{-1}$ ) to a doubly degenerate ( $E_g$ ) librational mode and the higher frequency, higher intensity band ( $270\text{--}345\text{ cm}^{-1}$ ) to a doubly degenerate ( $E_g$ ) translational mode (Fig. 1). The same assignments were made by White (1974a). Krishnamurti (1957) described the lattice modes as a mixture of part translational and part librational oscillations. Studies of  $\text{NaNO}_3$  (Rousseau et al., 1968), which crystallizes with the same symmetry as calcite, show that the lower frequency band of the Raman spectrum of  $\text{NaNO}_3$  is the translational mode and the higher frequency band is the librational mode of the nitrate ion, with little mixing between these modes. The behavior illustrated by the lattice bands of  $\text{NaNO}_3$  (higher frequency, higher intensity = libration) is generally expected from lattice bands of anisotropic groups (Bhagavantam, 1941). Rousseau et al. compared polarized Raman spectra of a single crystal of  $\text{NaNO}_3$  with the corresponding polarized spectra of calcite reported by Porto et al. (1966). On the basis of observed

differences in the polarization characteristics of calcite lattice bands, they suggested that considerable mixing is present in the lattice modes of calcite. At present, we will refer to the lower frequency mode as translational (T) and the higher frequency mode as librational (L), but realize that significant mixing may occur.

Because of the presence of alternating layers of calcium and magnesium ions in the dolomite structure, the symmetry of dolomite ( $R\bar{3}$ ) is lower than that of calcite. An additional lattice mode, which arises from translation of entire carbonate ions parallel to the  $c$  axis, occurs at approximately  $335\text{ cm}^{-1}$ . All of the other vibrational modes of the rhombohedral carbonates are found in the spectrum of dolomite (see White, 1974a, or Couture, 1947, for more detailed descriptions).

### Experimental procedures

Synthesis procedures for synthetic samples and pretreatment methods for biogenic samples are described by Bischoff et al. (1983). Results of atomic absorption and X-ray powder diffraction analyses of the materials can be found in Mackenzie et al. (1983) or are available from the authors.

Preparation of synthetic sample 25A differed from previous syntheses in that synthetic magnesite, instead of basic  $\text{MgCO}_3$  (hydromagnesite), was used in starting mixtures. This procedure eliminated previous problems of slight magnesium heterogeneities in run products with greater than 20 mol%  $\text{MgCO}_3$  (Bischoff et al., 1983). Run product 25A is a homogeneous phase, as indicated by a sharp, single-phase X-ray diffraction pattern. Because a small amount of periclase,  $\text{MgO}$ , was also produced in the synthesis of 25A, unit cell parameters determined from least squares analysis of the diffraction pattern were used with the X-ray determinative curves of Bischoff et al. (1983) to estimate the composition of 25A ( $25 \pm 1$  mol%  $\text{MgCO}_3$ ). Synthetic magnesite starting material was prepared in cold-seal bombs from Fisher reagent grade basic  $\text{MgCO}_3$  wrapped in Ag foil and subjected to a temperature of  $600^\circ\text{C}$  and a  $\text{CO}_2$  pressure of approximately 2000 psi for 48 hours.

Raman spectra were recorded at room temperature with a Spex 1402 double monochromator; data acquisition was controlled by a Spex Datamate computer. Powdered samples in glass capillaries were excited with a  $488.0\text{ nm}$   $\text{Ar}^+$  laser with a power of 200 mW at the sample. Scattered radiation was collected at  $90^\circ$  to the excitation beam. Only Stokes lines were recorded. A data collection interval of  $1\text{ cm}^{-1}$  and a slit width of 2 or  $3\text{ cm}^{-1}$  were used in recording Raman spectra.

### Experimental results

#### End members

Substitution of  $\text{Mg}^{2+}$  for  $\text{Ca}^{2+}$  in the synthetic and biogenic magnesian calcites is probably random. There is no evidence from X-ray powder diffraction studies of the samples considered here or elsewhere that magnesium ions are preferentially substituted into layers in a manner similar to that found in dolomite (Bischoff et al., 1983; Lippman, 1973). The true end members of the solid solution, thus, are calcite and magnesite. Nevertheless, we have included the Raman spectra of dolomite for comparison purposes and refer to it as an end member. Raman spectra of calcite, dolomite, and magnesite are shown in Figure 2. Fre-

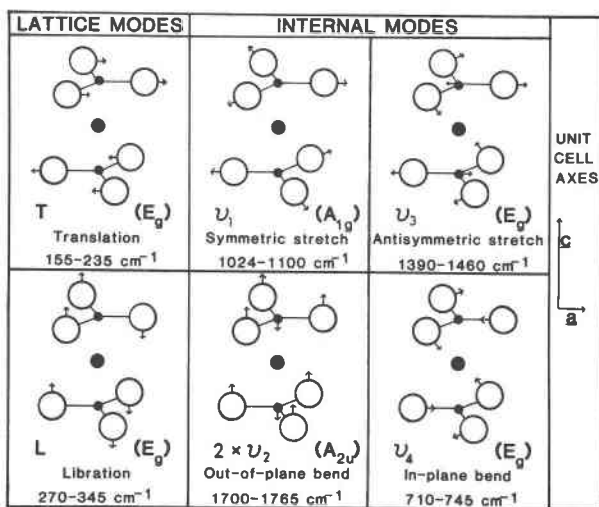


Fig. 1. Schematic drawings of Raman modes of vibration in rhombohedral carbonates (after White, 1974a). Notation and symmetry of the vibration and the range of Raman shift for all rhombohedral carbonates are included for each mode. Hexagonal unit cell axes are shown for orientation.

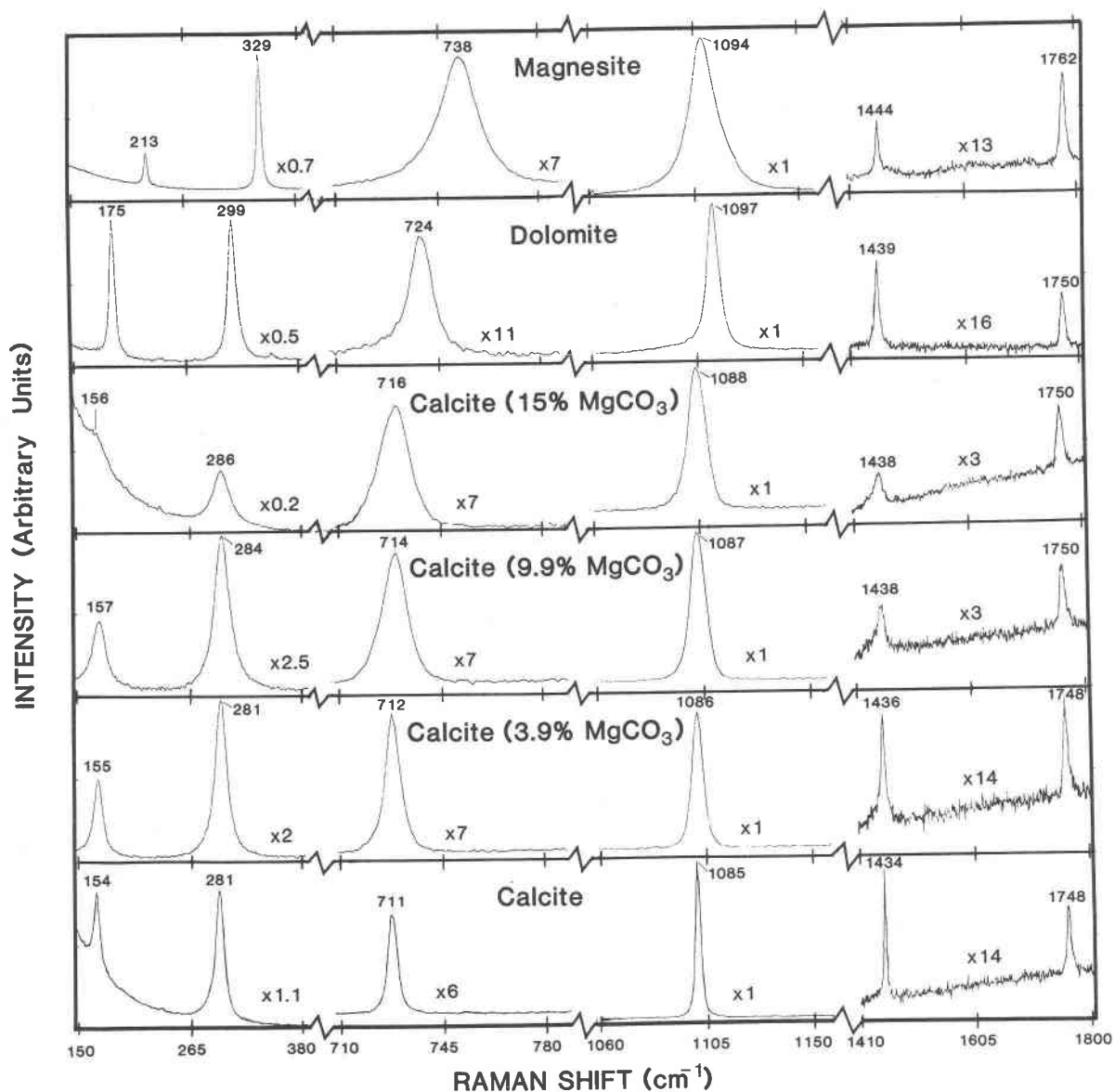


Fig. 2. Raman spectra of calcite, synthetic magnesian calcites, dolomite and magnesite. Percentages in parentheses refer to mol%  $\text{MgCO}_3$  in solid solution. Scale factors assume an intensity of 1 for the  $\nu_1$  mode of each sample.

quencies of vibrational modes of the end members agree well with other values reported in the literature, although literature values do show significant variation. The range of frequencies in literature values depends on the vibrational mode and is probably the result of variations in the natural materials studied as well as instrumental variation between investigators. References to the literature available on Raman spectra of carbonates, besides those cited here, can be found in the reviews by Griffith (1975), White (1974a), and Krishnan (1945).

Halfwidths of the Raman bands (full width of the Raman band at half maximum band height) were also recorded.

Halfwidths are a function of temperature, experimental slit width, the data recording interval, crystallinity of the sample (i.e., presence of structural defects and crystallite size), and substitution of trace elements. In this study, Raman spectra recording conditions were consistent, and differences in halfwidths reflect only variations between samples. Halfwidths of the internal modes generally increase from small values in calcite to considerably larger values found in magnesite. The halfwidths of the internal modes of dolomite fall between the values of calcite and magnesite (Table 1). For  $\nu_3$  the difference between dolomite and magnesite is not significant. This overall trend, how-

Table 1. Raman frequencies and halfwidths: synthetic phases and end members

Sample	Composition mole % MgCO <sub>3</sub> σ < 0.1	T	L	ν <sub>4</sub>	ν <sub>1</sub>	ν <sub>3</sub>	2xν <sub>2</sub>
Calcite		154* 6.2	281 10.1	711 3.6	1085 2.5	1434 2.0	1748 3.6
8C	1.9	155 8.2	281 12.0	711 4.8	1085 4.2	1435 6.4	1747 7.6
9B	3.9	155 10.7	281 13.8	712 5.9	1086 5.6	1436 7.6	1748 8.3
10C	5.7	155 11.5	282 15.6	712 7.4	1086 6.5	1436 10.2	1747 9.5
11A	8.0	156 13.3	284 15.1	714 8.7	1087 7.1	1438 11.4	1749 9.5
17A	9.9	157 14.7	284 18.3	714 9.7	1087 7.6	1438 14.0	1749 10.8
19C	12.5	156 15.9	283 20.0	714 12.2	1087 9.2	1438 17.8	1749 11.5
16B	15.0	156 im	286 18.3	716 12.2	1086 8.6	1439 19.1	1750 11.5
25A	25(1)	154 im	278 28.0	715 16.8	1088 12.4	1439 im	1748 15.3
Dolomite		175 5.5	299 9.8	724 9.0	1097 6.1	1441 3.8	1756 4.3
Magnesite		213 4.0	329 4.9	738 12.2	1093 12.5	1444 3.1	1762 4.8

\*Upper value is frequency, lower value is halfwidth. Errors are  $\pm 1 \text{ cm}^{-1}$  and  $< 0.5 \text{ cm}^{-1}$  for frequencies and halfwidths, respectively. im - Immeasurable because of degradation.

ever, suggests that cation size may play an important role in determining halfwidths of the internal modes of rhombohedral carbonates.

Magnesite has the smallest halfwidths of lattice modes and those of calcite are larger. Cation size also seems to be a factor controlling halfwidths of lattice modes, but in the opposite sense than the effect of cation size on the halfwidths of internal modes. Dolomite exhibits larger halfwidths of lattice bands than do magnesite or calcite. Halfwidths of the lattice modes of dolomite probably reflect the difference between vibrational energies of interactions of carbonate ions across layers of magnesium ions and those across layers of calcium ions.

The trends in the halfwidth data of both internal and lattice modes as a function of cation size probably arise from differences in bond strengths between calcite and magnesite. In both calcite and magnesite, C-O bond lengths in the carbonate ion are essentially the same, whereas the Ca-O bond in calcite (2.36Å) is larger and, thus, weaker than the Mg-O bond (2.10Å) in magnesite. Because the Mg-O bond in magnesite is stronger, there is less frequency variation in the lattice modes and the halfwidths are smaller than those for calcite. The halfwidths of the internal modes of calcite are smaller than those of magnesite because the weaker Ca-O bond has less effect on the internal vibrations of the carbonate ion than do the stronger Mg-O bonds in magnesite.

These interpretations of the halfwidth behavior of the

end member carbonates should be considered preliminary. Raman spectra of a variety of samples of calcite, dolomite and magnesite should be recorded under consistent experimental conditions to determine if these halfwidth relationships apply to these (and other rhombohedral) carbonates in general. The halfwidths of the Raman bands of calcite reported here, however, do agree within  $2 \text{ cm}^{-1}$  of similar values reported by Krishnan (1945) and Park (1966). In a study of magnesite, Krishnamurti (1956) described the halfwidth of the L lattice mode as sharp and that of the  $\nu_1$  mode as diffuse ( $\sim 10 \text{ cm}^{-1}$ ). We conclude that the limited halfwidth data available suggest that the observed halfwidth trends are real, and not the result of peculiarities in our samples.

### Synthetic materials

Raman spectra for a selection of synthetic magnesian calcites are also shown in Figure 2. Careful examination of Figure 2 reveals that the frequencies of all the Raman bands in the spectra of synthetic materials generally appear to increase slightly with increasing magnesium concentration. To investigate these relationships more closely, we plotted Raman frequencies against mol% MgCO<sub>3</sub> and constructed straight lines between calcite and dolomite and calcite and magnesite (Figs. 3 and 4). These lines have an error of at least  $\pm 1 \text{ cm}^{-1}$ , the error in measurement of Raman frequencies of the end members. Actual error may be greater because of the ranges in frequencies reported for the end members in the literature (see discussion above). When we exclude the results from sample 25A, and within the error of measurement of  $\pm 1 \text{ cm}^{-1}$ , Raman frequencies of synthetic phases plot along the straight lines drawn be-

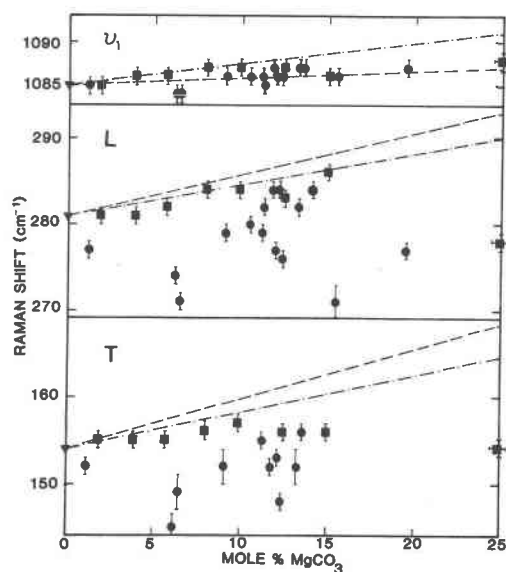


Fig. 3. Frequencies of the  $\nu_1$ , L and T Raman modes vs. composition of synthetic (squares) and biogenic (circles) magnesian calcites. Dot-dashed line connects calcite (triangle) and dolomite. Dashed line connects calcite and magnesite.

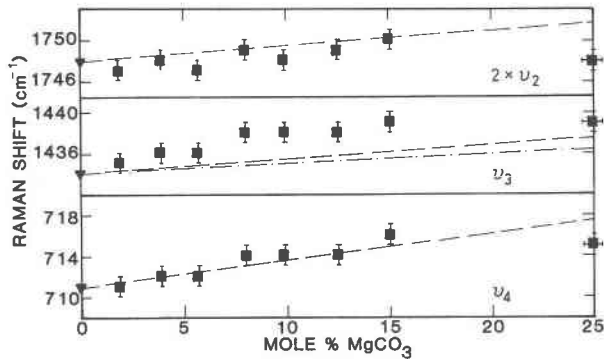


Fig. 4. Frequencies of the  $\nu_4$ ,  $\nu_3$ , and  $2 \times \nu_2$  Raman modes vs. composition for synthetic magnesian calcites. Lines and symbols are the same as in Fig. 3, but lines to dolomite and magnesite are superimposed for the  $2 \times \nu_2$  and  $\nu_4$  modes.

tween calcite and dolomite or calcite and magnesite for the L,  $\nu_1$ ,  $\nu_4$  and  $2 \times \nu_2$  modes. Positive deviations from the straight lines are seen for the  $\nu_3$  mode and negative deviations for the T mode. Sample 25A complements the trends determined by other synthetic phases found in the internal modes except in the case of the  $2 \times \nu_2$  mode, where the frequency falls  $2 \text{ cm}^{-1}$  below that expected for a synthetic magnesian calcite of 25 mol%  $\text{MgCO}_3$ . The frequencies of the lattice modes of sample 25A are anomalous. These frequencies are equivalent (for the T mode) or below (for the L mode) the corresponding frequencies of calcite. Frequencies of the Raman bands and associated halfwidths are given in Table 1.

Halfwidths of the Raman bands of synthetic phases also increase with increasing magnesium concentration. An increase in halfwidth can eventually lead to complete degradation of Raman bands. In Figure 2, this effect is noticeable in the lattice modes of the synthetic phases. The increase in halfwidths, as a function of magnesium concentration, appears linear for all modes, but is more pronounced in lattice modes than in internal modes. The halfwidths in the spectrum of sample 25A complement the trends determined by the other synthetic phases in each mode. Halfwidths of the  $\nu_1$  and L modes, as a function of magnesium concentration, are plotted in Figure 5. All halfwidths of Raman bands of synthetic phases are given in Table 1.

#### Biogenic samples

Figure 6 depicts Raman spectra obtained for a selection of biogenic magnesian calcites. The internal modes of biogenic phases generally show increases in frequencies of Raman bands with increasing magnesium concentrations, but the trend is not nearly as smooth as that found for synthetic phases (Fig. 3). Many of the biogenic phases have frequencies of translational and librational modes that are lower than those of calcite. Also, the halfwidths of the Raman bands of biogenic phases are all greater than those of synthetic phases of similar composition, regardless of magnesium concentration, with the exception of synthetic

sample 25A (Fig. 5). Several of the biogenic phases lack discernible Raman bands of the translational mode. In the case of *Lithothamnium corallioides*, even the more intense librational mode is degraded beyond measurement above background levels (Table 2).

Many biogenic materials exhibit Raman bands at  $\sim 1014 \text{ cm}^{-1}$ , indicating the presence of bicarbonate ( $\text{HCO}_3^-$ ) ions. In these specimens,  $\text{HCO}_3^-$  concentrations are on the order of 500–3000 ppm and may provide a charge balance mechanism for comparable amounts of  $\text{Na}^+$  found in many biogenic skeletons (Bischoff et al., 1983; White, 1975; Veizer, 1983).

Incorporation of trace amounts of transition metal ions can result in fluorescence from the sample when it is excited with a laser beam. Generally, all biogenic materials contain fluorescent metal ions (Bischoff et al., 1983; Veizer, 1983) and nearly all of the biogenic specimens observed showed some fluorescence that was commonly strong enough to obscure some of the weak Raman bands (Fig. 6).

#### Chemical and structural interpretations

Because substitution of  $\text{Mg}^{2+}$  for  $\text{Ca}^{2+}$  is random in the magnesian calcite solid solution, there is no loss of rotational symmetry. Factor group analysis predicts that members of the solid solution should have Raman spectra like those of the end members, but with a continual shift in frequency between the end members as the composition is varied (White, 1974b). This behavior is exhibited by the synthetic magnesian calcites, except for the lattice modes of sample 25A. Raman shifts increase from calcite to magnesite because the magnesium ion is smaller than the calcium ion. Substitution of magnesium for calcium results in a decrease in interatomic distances and a subsequent increase in the vibrational frequencies of the carbonate ion (Krishnamurti, 1956; White 1974a). Raman shifts are mostly controlled by the crystal field; significant changes in

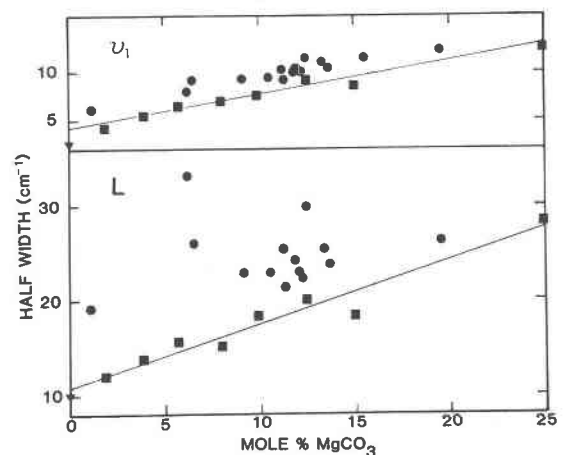


Fig. 5. Halfwidths of the  $\nu_1$  and L Raman modes vs. composition for synthetic (squares) and biogenic (circles). Calcite is represented by the triangle. Least-squares line drawn through synthetic phases for reference.

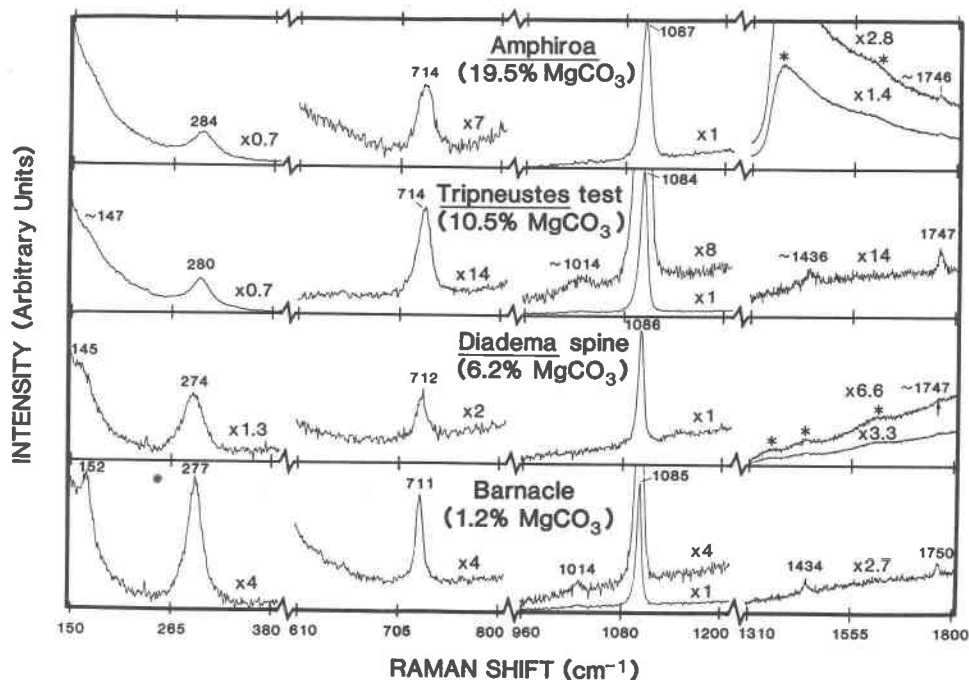


Fig. 6. Raman spectra of biogenic magnesian calcites. Explanation is the same as for Figure 2. Asterisks (\*) mark fluorescence bands. The weak band at  $\sim 1014 \text{ cm}^{-1}$  arises from bicarbonate ( $\text{HCO}_3^-$ ).

C–O bond lengths are not seen in rhombohedral carbonates (Effenberger et al., 1981; Reeder, 1983), whereas significant differences in Raman frequency are observed as a function of cation size (White, 1974a; Rutt and Nicola, 1974).

Random substitution of magnesium for calcium results in differences in the immediate cation neighborhood of carbonate ions. These differences account, in part, for the increase in line widths of Raman bands as a function of magnesium concentration, particularly as seen in the internal modes of the synthetic and biogenic phases.

The Raman spectra of biogenic magnesian calcites and synthetic sample 25A show different behavior in their Raman spectra in contrast to the synthetic phases with concentrations of magnesium less than 16 mol%  $\text{MgCO}_3$ . Raman spectra of many of the biogenic samples and sample 25A are characterized by very low frequencies and large halfwidths of lattice modes (Figs. 3 and 5). The low frequencies of the lattice modes suggest that biogenic phases may have large, open unit cells. Many studies have shown, however, that cell volumes of biogenic magnesian calcites decrease with magnesium concentration (Chave, 1952, 1954a; Goldsmith et al., 1955; Milliman et al., 1971; Bischoff et al., 1983). If the low frequencies recorded for many of the biogenic magnesian calcites and sample 25A were a function of their unit cell size, unit cells larger than that for calcite would be required for these phases.

Inhomogeneities in magnesium concentration could give rise to the large halfwidths found in biogenic magnesian calcites. Most specimens, however, exhibit ranges in mag-

nesium concentration only slightly larger than those found in synthetic phases as determined by electron microprobe analysis. (Synthetic and biogenic materials have ranges of  $\pm 0.4$ – $0.7$  and  $\pm 0.5$ – $1.2$  mol%  $\text{MgCO}_3$ , respectively). There is no correlation between ranges of magnesium concentration and halfwidths, but magnesium heterogeneities probably contribute slightly to the degradation of the lattice bonds and the larger halfwidths of bands of internal modes of biogenic phases. *Lithothamnium corallioides* and *Amphiroa rigida* are exceptions. Electron microprobe analyses of these biogenic magnesian calcites indicated large inhomogeneities in magnesium concentration of  $\sim 10$  mol%  $\text{MgCO}_3$  (Bischoff et al., 1983). Magnesium inhomogeneities may contribute significantly to the degradation of lattice bands (and bands of internal modes in the case of *Lithothamnium corallioides*) observed in the Raman spectra of these phases.

Substitution of trace elements cannot account for the large halfwidths observed in the spectra of biogenic phases. No correlation exists between trace element concentrations, as determined by electron microprobe analyses (Bischoff et al., 1983), and halfwidths of Raman bands. Slight increases in halfwidths, however, may arise from the incorporation of trace elements.

We favor a mechanism of positional disorder of the carbonate ion to explain the behavior of the Raman bands of biogenic phases and synthetic sample 25A. In end member rhombohedral carbonates, layers of "flat" carbonate ions are separated by layers of cations along the hexagonal c axis. Carbonate ions are similarly oriented within each

Table 2. Raman frequencies and halfwidths: biogenic phases

Specimen	Composition mole % MgCO <sub>3</sub> σ < 0.1	T	L	ν <sub>4</sub>	ν <sub>1</sub>
Barnacle	1.2	152* 13.9	277 19.2	711 8.2	1085 6.0
<u>Diadema antillarum</u> (spine, specimen 1)	6.2	145(2) im	274 33.1	712 8.2	1084 8.0
<u>Lytechinus variegatus</u> (spine, specimen 1)	6.5	149(2) im	271 26.1	710 10.7	1084 9.2
<u>Diadema antillarum</u> (spine tip, specimen 1)	9.1	152(2) im	279 22.9	712 14.8	1086 9.7
<u>Tripneustes esculentis</u> (test)	10.5	im	280 22.9	714 15.0	1086 9.5
<u>Lytechinus variegatus</u> (test, specimen 2)	11.2	im	279 25.4	nr	1086 10.4
<u>Lytechinus variegatus</u> (teeth, specimen 1)	11.3	155 15.3	282 21.3	713 12.2	1085 9.2
<u>Diadema antillarum</u> (test, specimen 1)	11.8	152 20.4	284 24.2	nr	1087 9.9
<u>Lytechinus variegatus</u> (test, specimen 1)	12.0	im	277 23.0	713 15.8	1086 10.2
<u>Diadema antillarum</u> (test, specimen 2)	12.2	153 26.4	284 22.3	715 13.4	1087 10.1
<u>Homotrema rubrim</u>	12.4	148 im	276 29.9	712 16.3	1085 11.6
<u>Echinometra lucanter</u> (teeth)	13.3	152(2) im	282 25.0	714 17.3	1087 11.2
<u>Echinometra lucanter</u> (test)	13.6	157 21.0	284 23.8	715 15.3	1087 10.7
<u>Lithothamnium corallioides</u>	15.5	im	270(2) im	nr	1086 11.7
<u>Amphiroa rigida</u>	19.5	im	277 26.2	714 16.8	1087 12.4

\*Upper value is frequency, lower value is halfwidth. Errors are  $\pm 1 \text{ cm}^{-1}$  and  $< 0.5 \text{ cm}^{-1}$  for frequencies and halfwidths, respectively, except where noted.  
im - Immeasurable because of degradation. nr - Not recorded.

layer, but the orientation is reversed in alternate carbonate layers. The hexagonal *a* axes lie within the planes formed by the cation (or anion) layers (cf. Reeder, 1983). Any mechanism of anion disorder would affect the behavior of Raman bands, but consideration of the results of unit cell refinements suggests that the mechanism of anion disorder obtaining in magnesian calcites is one in which carbonate ions are rotated out of planes parallel to the *a* axes into the direction of the *c* axis.

The *c/a* axial ratios of synthetic magnesian calcites describe a smooth curve as a function of magnesium concentration exhibiting positive deviation from the "ideal" straight line connecting calcite and least-ordered dolomite or magnesite (Bischoff et al., 1983; Mackenzie et al., 1983). Positional disorder, as a function of magnesium concentration, is a mechanism that is likely to give rise to the observed axial ratio behavior. Positional disorder obtains

in the vicinity of magnesium ions to allow for shorter Mg-O bonding. The largest deviation of *c/a* ratio from the ideal occurs at approximately 25 mol% MgCO<sub>3</sub>. At concentrations greater than 25 mol% MgCO<sub>3</sub>, substitution of several magnesium ions in the immediate anion neighborhood (in cation planes above and below the layer of anions) may prevent positional disorder. The deviation of *c/a* ratios from the straight-line relationship diminishes with increasing MgCO<sub>3</sub> concentration above 25 mol%. The large amount of positional disorder in sample 25A accounts for the large halfwidths observed and low frequencies of the lattice mode bands.

Bischoff et al. (1983) also found that biogenic magnesian calcites generally have unit cell volumes and *c/a* axial ratios larger than synthetic phases of similar magnesium concentrations. The larger cell volumes of biogenic phases indicate that some mechanism of disorder probably occurs



in these phases. The variation of unit cell volumes,  $c/a$  axial ratios, and Raman band halfwidths and frequencies of lattice modes in biogenic phases is not as smooth a function of magnesium concentration as it is for synthetic phases. Generally, biogenic phases exhibit more positional disorder than synthetic phases of similar magnesium concentration. The differences observed between biogenic and synthetic phases, however, are probably a function of magnesium heterogeneity and trace element substitution, as well as positional disorder in excess of that in synthetic phases.

The possibility of positional disorder obtaining in magnesian calcites was suggested originally by Lippmann (1973). He noted that in huntite,  $Mg_3Ca(CO_3)_4$ , only carbonate ions solely bonded to magnesium did not show "tilt" out of the basal ( $a$  axes) planes. All other carbonate groups in this structure are tilted out of the basal plane to provide shorter Mg-O bonds. Lippmann suggested that similar "tilting" mechanisms might occur in magnesian calcites because of magnesium substitution.

In a discussion of the "modulated structures" seen in many TEM analyses of calcite and dolomite, Wenk et al. (1983) suggested that these structures may arise from periodic reversals in the orientation of carbonate ions within the basal plane. This rotational disorder probably is accompanied by "tilting" of carbonate ions out of the basal plane in the vicinity of the defects.

A possible interpretation of an X-ray crystal structure refinement done by Althoff (1977) on an echinoid test is that positional disorder obtains in this magnesian calcite. On the basis of the thermal parameters of the echinoid investigated by Althoff, Reeder (1983) found that the root mean square amplitudes for the principal axes of the vibrational ellipsoids are roughly 40–50% greater than those in calcite. He suggested that whereas it is not unlikely to have greater thermal vibrations in solid solution, these greater thermal vibrations probably reflect some positional disorder. If positional disorder occurs in the vicinity of substituted magnesium ions, averaging the thermal vibrations over the whole structure by single crystal X-ray diffraction would increase the value of the thermal parameters.

### Conclusions

Raman spectra of synthetic magnesian calcites show behavior expected from factor group analysis. Raman frequencies of synthetic phases lie between the values for calcite and magnesite and shift as a function of magnesium concentration. The halfwidths of Raman bands also increase as a function of magnesium content. Part of the increase in halfwidths arises from substitution of  $Mg^{2+}$  for  $Ca^{2+}$  and the subsequent differences in the immediate cation neighborhood of carbonate anions. The increase in halfwidths, however, is primarily the result of positional disorder of the carbonate ion. The amount of positional disorder present in synthetic phases is a function of magnesium concentration, as suggested from analysis of  $c/a$  axial ratios. Of the synthetic phases studied, sample 25A, containing 25 mol%  $MgCO_3$ , shows the greatest amount of positional disorder which accounts for its very large

halfwidths and, probably, the anomalously low frequencies of its lattice modes.

Biogenic magnesian calcites generally exhibit larger halfwidths and lower frequencies of lattice modes than synthetic phases of similar magnesium concentrations. This behavior of lattice modes arises in part from the presence of positional disorder in excess of that found in synthetic phases but probably also from magnesium heterogeneities and substitution of trace elements. The fact that biogenic phases generally have larger unit cell volumes and  $c/a$  ratios than synthetic phases of similar magnesium concentration suggests that positional disorder is the major contributing factor to the larger halfwidths and low frequencies of lattice modes. The presence of trace transition metal ions and bicarbonate ions is detectable by the occurrence of fluorescence and a Raman band at  $1014\text{ cm}^{-1}$ , respectively, in the Raman spectra of biogenic phases.

The presence of positional disorder of the carbonate ion in magnesian calcite has not been previously recognized. It is likely that positional disorder is an important factor to consider when modeling the solid solution behavior of magnesian calcites at earth surface temperatures and pressures. Complete knowledge of the thermodynamic properties of magnesian calcite is essential for an understanding of the widespread occurrence and diagenetic behavior of magnesian calcite skeletal materials and cements.

### Acknowledgments

We gratefully acknowledge Jane Schoonmaker, Keith Chave and especially Rich Reeder for critically reviewing the manuscript. We thank Murlu Manghnani for access to the  $Ar^+$  laser and Carol Koyanagi and Pat Sexton for typing the manuscript. Funding for the Spex Datamate computer was provided by NSF Grant EAR80-26091 (SKS). This work is supported by NSF Grants EAR82-19513 (FTM) and EAR82-13720 (Finley C. Bishop, Northwestern University). Hawaii Institute of Geophysics Contribution No. 1583.

### References

- Althoff, P. L. (1977) Structural refinements of dolomite and a magnesian calcite and implications for dolomite formation in the marine environment. *American Mineralogist*, 62, 772–783.
- Bathurst, R. G. C. (1975) *Carbonate Sediments and Their Diagenesis*, 2nd edition. Elsevier, Amsterdam.
- Bhagavantam, S. (1941) Raman effect in relation to crystal structure: Lattice oscillations. *Proceedings of the Indian Academy of Sciences*, A13, 543–563.
- Bhagavantam, S. and Venkatarayudu, T. (1939) Raman effect in relation to crystallographic structure. *Proceedings of the Indian Academy of Sciences*, A9, 224–258.
- Bischoff, W. D., Bishop, F. C., and Mackenzie, F. T. (1983) Biogenically produced magnesian calcites: Inhomogeneities in chemical and physical properties; comparison with synthetic phases. *American Mineralogist*, 68, 1183–1188.
- Chave, K. E. (1952) A solid solution between calcite and dolomite. *Journal of Geology*, 60, 190–192.
- Chave, K. E. (1954a) Aspects of the biogeochemistry of magnesium. 1. Calcareous marine organisms. *Journal of Geology*, 62, 266–283.
- Chave, K. E. (1954b) Aspects of the biogeochemistry of mag-



- nesium. 2. Calcareous sediments and rocks. *Journal of Geology*, 62, 587–599.
- Couture, Lucienne (1947) Etudes des spectres de vibrations de monocristaux ioniques. *Annales de Physique (Paris)*, 17, 88–122.
- Effenberger, H., Mereiter, K., and Zemann, J. (1981) Crystal structure refinements of magnesite, calcite, rhodochrosite, siderite, smithsonite and dolomite, with discussion of some aspects of the stereochemistry of calcite-type carbonates. *Zeitschrift für Kristallographie*, 156, 233–243.
- Griffith, W. P. (1975) Raman spectroscopy of terrestrial minerals. In C. Karr, Jr., Ed., *Infrared and Raman Spectroscopy of Lunar and Terrestrial Materials*, p. 299–323. Academic, New York.
- Goldsmith, J. R., Graf, D. L., Joensuu, O. I. (1955) The occurrence of magnesian calcites in nature. *Geochimica et Cosmochimica Acta*, 7, 212–230.
- Krishnamurti, D. (1956) Raman spectrum of magnesite. *Proceedings of the Indian Academy of Sciences*, A43, 210–212.
- Krishnamurti, D. (1957) The Raman spectrum of calcite and its interpretation. *Proceedings of the Indian Academy of Sciences*, A46, 183–202.
- Krishnan, R. S. (1945) Raman spectra of the second order in crystals. Part 1. Calcite. *Proceedings of the Indian Academy of Sciences*, A22, 182–193.
- Land, L. S. (1967) Diagenesis of skeletal carbonates. *Journal of Sedimentary Petrology*, 37, 914–930.
- Lippmann, Friedrich (1973) *Sedimentary Carbonate Minerals*. Springer-Verlag, New York.
- Mackenzie, F. T., Bischoff, W. D., Bishop, F. C., Loijens, Michele, Schoonmaker, Jane, and Wollast, Roland (1983) Magnesian calcites: Low-temperature occurrence, solubility, and solid solution behavior. In R. J. Reeder, Ed., *Carbonates: Mineralogy and Chemistry*. *Reviews in Mineralogy*, 11, p. 97–144. Mineralogical Society of America, Washington.
- Milliman, J. D., Gastner, Manfred, and Muller, Jens (1971) Utilization of magnesium in coralline algae. *Geological Society of America Bulletin*, 82, 573–580.
- Park, K. (1966) New width data of the  $A_{1g}$  Raman line in calcite. *Physics Letters*, 22, 39–41.
- Porto, S. P. S., Giordmaine, J. A., and Damen, T. C. (1966) Depolarization of Raman scattering in calcite. *Physical Review*, 147, 608–611.
- Reeder, R. J. (1983) Crystal chemistry of the rhombohedral carbonates. In R. J. Reeder, Ed., *Carbonates: Mineralogy and Chemistry*. *Reviews in Mineralogy*, 11, p. 1–48. Mineralogical Society of America, Washington.
- Rousseau, D. L., Miller, R. F., and Leroi, G. E. (1968) Raman spectrum of crystalline sodium nitrate. *Journal of Chemical Physics*, 48, 3409–3413.
- Rutt, H. N. and Nicola, J. H. (1974) Raman spectra of carbonates of calcite structure. *Journal of Physics, C: Solid State Physics*, 7, 4522–4528.
- Veizer, Jan (1983) Trace elements and isotopes in sedimentary carbonates. In R. J. Reeder, Ed., *Carbonates: Mineralogy and Chemistry*. *Reviews in Mineralogy*, 11, p. 265–300. Mineralogical Society of America, Washington.
- Wenk, H.-R., Barber, D. J., and Reeder, R. J. (1983) Microstructures in carbonates. In R. J. Reeder, Ed., *Carbonates: Mineralogy and chemistry*. *Reviews in Mineralogy*, 11, p. 301–367. Mineralogical Society of America, Washington.
- White, A. F. (1975) Sodium and Potassium Coprecipitation in Calcium Carbonate. Ph.D. Thesis, Northwestern University, Evanston.
- White, W. B. (1974a) The carbonate minerals. In V. C. Farmer, Ed., *The Infra-red Spectra of Minerals*. Mineralogical Society Monograph 4, p. 227–284. Mineralogical Society, London.
- White, W. B. (1974b) Order-disorder effects. In V. C. Farmer, Ed., *The Infra-red Spectra of Minerals*. Mineralogical Society Monograph 4, p. 87–110. Mineralogical Society, London.

*Manuscript received, May 14, 1984;  
accepted for publication, January 7, 1985.*